Finite matrix crack penetrating
a partially debonded circular inhomogeneity

X. WANG[1)], P. SCHIAVONE[2)]

[1)] *School of Mechanical and Power Engineering*
East China University of Science and Technology
130 Meilong Road, Shanghai 200237, China

[2)] *Department of Mechanical Engineering*
University of Alberta
4–9 Mechanical Engineering Building
Edmonton, Alberta Canada T6G 2G8
e-mail: P.Schiavone@ualberta.ca

WE RIGOROUSLY SOLVE THE PROBLEM of a finite matrix crack penetrating a partially debonded circular elastic inhomogeneity under longitudinal shear. The tips of the matrix crack are mutual image points with respect to the inhomogeneity/matrix interface and one tip of the interface crack is located at the intersection point between the matrix crack and the circular interface. Closed-form expressions of mode-III stress intensity factors at all three crack tips as well as displacement jumps across the crack surfaces are obtained. Our results are illustrated in graphical form and verified by comparison with existing results in the literature.

Key words: matrix crack, interfacial debonding, stress intensity factors, displacement jumps.

1. Introduction

INTERFACIAL DEBONDING AND MATRIX CRACKING, both known to be major failure modes in fibrous composites, have received considerable attention in the literature (see, for example, [1, 2, 4, 5, 7–9, 11–15]). If one tip of a matrix crack is located at the interface, it is of interest to ask if the crack will further penetrate the fiber (or inhomogeneity) or deflect into the interface itself. In several previous investigations of this matter (see, for example, [2, 9, 13–15]), in order to simplify the analysis, it was assumed that the crack will penetrate only the inhomogeneity and not cause any interfacial debonding. This simplified scenario is based on the premise that the interface is sufficiently tough to prevent any interface debonding [3].

In this work, we will consider the more complex, realistic and challenging situation in which interfacial debonding results from a radial matrix crack pene-

trating a circular inhomogeneity. Interestingly, closed-form solutions can still be derived when the two tips of the radial crack are simply mutual image points with respect to the circular interface, and when the fibrous composite is subjected to longitudinal shear.

The paper is ordered as follows. In Section 2, we first derive an analytic solution for the case when the loading corresponds to the matrix being subjected to only remote uniform anti-plane shear stresses. Fracture parameters such as stress intensity factors and displacement jumps across the crack surfaces for this particular case are then given in Section 3. Discussions and numerical results are presented in Section 4 to demonstrate the closed-form expressions obtained in Section 3. Finally in Section 5, we derive analytic solutions for three other loading cases: (i) when the radial crack and arc interface crack form a Zener–Stroh crack; (ii) when a screw dislocation is located in the matrix; and (iii) when a screw dislocation is located within the inhomogeneity.

2. Analytic solution

Under anti-plane shear deformation, the out-of-plane displacement w, the stress function ϕ, and the stress components σ_{zy} and σ_{zx} can be expressed in terms of a single analytic function $f(z)$ of the complex variable $z = x + \mathrm{i}y = r\exp(\mathrm{i}\theta)$ as

$$\mu^{-1}\phi + \mathrm{i}w = f(z), \qquad \sigma_{zy} + \mathrm{i}\sigma_{zx} = \mu f'(z),$$

where μ is the shear modulus. The two stress components σ_{zy} and σ_{zx} can be expressed in terms of the stress function ϕ as

$$\sigma_{zy} = \phi_{,x}, \qquad \sigma_{zx} = -\phi_{,y}.$$

As shown in Fig. 1, we consider an infinite matrix described by $S_2 : x^2 + y^2 \geq 1$ reinforced by a circular elastic inhomogeneity of unit radius denoted by $S_1 : x^2 + y^2 \leq 1$. A radial matrix crack on the real axis penetrates the circular inhomogeneity and causes interfacial debonding on the arc L_c. The right tip of the radial crack is located at $z = a$, $a > 1$, while its left tip is located at $z = 1/a$. One tip of L_c is at $z = 1$ with the other at $z = \exp(\mathrm{i}\theta_0)$, $(0 \leq \theta_0 \leq 2\pi)$. The matrix is subjected to remote uniform anti-plane shear stresses σ_{zy}^∞ and σ_{zx}^∞.

In order to solve this problem, we introduce the following conformal mapping function

$$z = \omega(\xi) = \frac{a\xi^2 + 1}{\xi^2 + a}, \qquad \xi(z) = u + \mathrm{i}v = -\sqrt{\frac{1 - az}{z - a}}, \qquad \mathrm{Im}\{\xi\} \leq 0,$$

which maps the circular inhomogeneity onto $|\xi| \leq 1$, $\mathrm{Im}\{\xi\} \leq 0$, and maps the matrix onto $|\xi| \geq 1$ with $\mathrm{Im}\{\xi\} \leq 0$ (see Fig. 2). In addition the finite crack
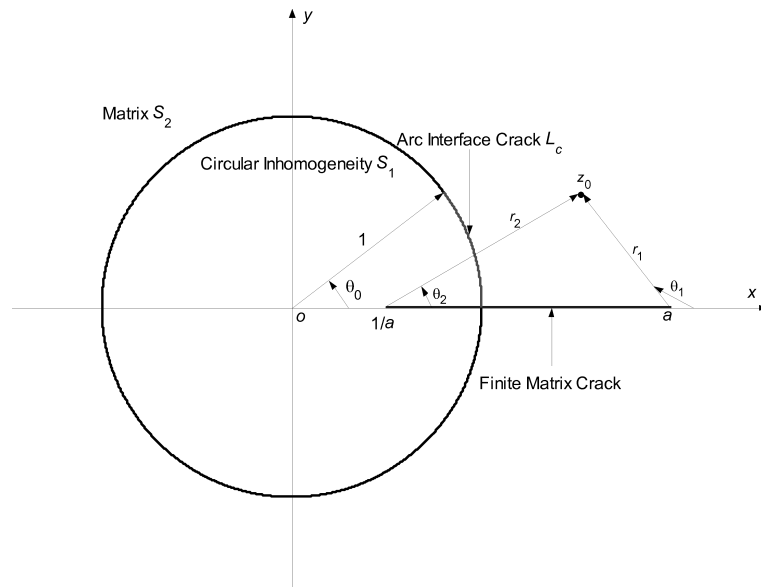
FIG. 1. A finite matrix crack penetrating a partially debonded circular inhomogeneity.
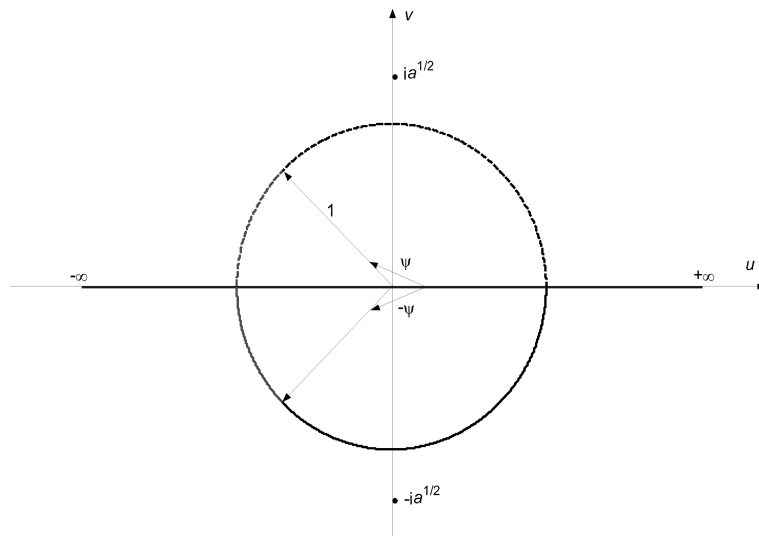
FIG. 2. The problem in the mapped ξ-plane.

described by $x \in [1/a, a]$ and $y = 0$ is mapped to $-\infty < \mathrm{Re}\{\xi\} < +\infty$ and $\mathrm{Im}\{\xi\} = 0$; the tip of the interface crack L_c at $z = 1$ is mapped to $\xi = -1$ while the other tip at $z = \exp(i\theta_0)$ is mapped to $\xi = \exp(-i\psi)$, $(0 \leq \psi \leq \pi)$. Finally, $z = \infty$ is mapped to the point $\xi = -i\sqrt{a}$. In the following we will en-

deavor to derive the two analytic functions: $f_1(\xi) = f_1(\omega(\xi))$ with $|\xi| \leq 1$ and $\text{Im}\{\xi\} \leq 0$ for the circular inhomogeneity and $f_2(\xi) = f_2(\omega(\xi))$ with $|\xi| \geq 1$ and $\text{Im}\{\xi\} \leq 0$ for the unbounded matrix. Due to the action of the remote uniform stresses σ_{zy}^∞ and σ_{zx}^∞, the analytic function $f_2(\xi)$ has a first-order pole at $\xi = -\text{i}\sqrt{a}$: $(a^{3/2} - a^{-1/2})(\sigma_{zx}^\infty - \text{i}\sigma_{zy}^\infty)/2\mu_2(\xi + \text{i}\sqrt{a})$. If we add another (imaginary) pole for $f_2(\xi)$ at $\xi = \text{i}\sqrt{a}$: $-(a^{3/2} - a^{-1/2})(\sigma_{zx}^\infty + \text{i}\sigma_{zy}^\infty)/2\mu_2(\xi - \text{i}\sqrt{a})$, the original half ξ-plane can be extended to the whole ξ-plane as shown in Fig. 2. Now only the following interface conditions at $|\xi| = 1$ are left to be satisfied:

$$(2.1) \qquad \begin{aligned} f_1(\xi) - \overline{f_1(\xi)} &= f_2(\xi) - \overline{f_2(\xi)}, \\ \mu_1 f_1(\xi) + \mu_1 \overline{f_1(\xi)} &= \mu_2 f_2(\xi) + \mu_2 \overline{f_2(\xi)}, \end{aligned}$$

for $|\xi| = 1$ and $-\psi < \arg(\xi) < \psi$,

$$(2.2) \qquad \mu_1 f_1(\xi) + \mu_1 \overline{f_1(\xi)} = \mu_2 f_2(\xi) + \mu_2 \overline{f_2(\xi)} = 0,$$

for $|\xi| = 1$ and $\psi < \arg(\xi) \leq \pi$, $-\pi \leq \arg(\xi) < -\psi$.

Condition (2.1) is due to the fact that displacement and traction are both continuous across the bonded part of the circular interface, whilst condition (2.2) is the traction-free condition on the debonded part L_c of the circular interface.

Using analytic continuation, the boundary value problem (2.1) and (2.2) can be finally reduced to a standard Riemann–Hilbert problem with discontinuous coefficients [6]. Thus the two analytic functions $f_1(\xi)$ and $f_2(\xi)$ can be conveniently derived as

$$f_1(\xi) = \frac{1}{2(\mu_1 + \mu_2)} \left[\begin{array}{c} \dfrac{(a^{\frac{3}{2}} - a^{-\frac{1}{2}})(\sigma_{zx}^\infty - \text{i}\sigma_{zy}^\infty)}{\xi + \text{i}a^{\frac{1}{2}}} - \dfrac{(a^{\frac{3}{2}} - a^{-\frac{1}{2}})(\sigma_{zx}^\infty + \text{i}\sigma_{zy}^\infty)}{\xi - \text{i}a^{\frac{1}{2}}} \\[2mm] -\dfrac{(a^{\frac{1}{2}} - a^{-\frac{3}{2}})(\sigma_{zx}^\infty + \text{i}\sigma_{zy}^\infty)}{\xi + \text{i}a^{-\frac{1}{2}}} + \dfrac{(a^{\frac{1}{2}} - a^{-\frac{3}{2}})(\sigma_{zx}^\infty - \text{i}\sigma_{zy}^\infty)}{\xi - \text{i}a^{-\frac{1}{2}}} \end{array} \right]$$

$$+ \frac{\sqrt{(\xi - \text{e}^{\text{i}\psi})(\xi - \text{e}^{-\text{i}\psi})}}{2(\mu_1 + \mu_2)} \times$$

$$\left[\begin{array}{c} \dfrac{(a^{\frac{3}{2}} - a^{-\frac{1}{2}})(\sigma_{zx}^\infty - \text{i}\sigma_{zy}^\infty)}{\sqrt{(-\text{i}a^{\frac{1}{2}} - \text{e}^{\text{i}\psi})(-\text{i}a^{\frac{1}{2}} - \text{e}^{-\text{i}\psi})}(\xi + \text{i}a^{\frac{1}{2}})} - \dfrac{(a^{\frac{3}{2}} - a^{-\frac{1}{2}})(\sigma_{zx}^\infty + \text{i}\sigma_{zy}^\infty)}{\sqrt{(\text{i}a^{\frac{1}{2}} - \text{e}^{\text{i}\psi})(\text{i}a^{\frac{1}{2}} - \text{e}^{-\text{i}\psi})}(\xi - \text{i}a^{\frac{1}{2}})} + \\[3mm] \dfrac{(a^{\frac{1}{2}} - a^{-\frac{3}{2}})(\sigma_{zx}^\infty + \text{i}\sigma_{zy}^\infty)}{\sqrt{(-\text{i}a^{-\frac{1}{2}} - \text{e}^{\text{i}\psi})(-\text{i}a^{-\frac{1}{2}} - \text{e}^{-\text{i}\psi})}(\xi + \text{i}a^{-\frac{1}{2}})} - \dfrac{(a^{\frac{1}{2}} - a^{-\frac{3}{2}})(\sigma_{zx}^\infty - \text{i}\sigma_{zy}^\infty)}{\sqrt{(\text{i}a^{-\frac{1}{2}} - \text{e}^{\text{i}\psi})(\text{i}a^{-\frac{1}{2}} - \text{e}^{-\text{i}\psi})}(\xi - \text{i}a^{-\frac{1}{2}})} \end{array} \right],$$

$|\xi| \leq 1$ and $\text{Im}\{\xi\} \leq 0$;

$$f_2(\xi) = \frac{1}{2(\mu_1+\mu_2)}\left[\begin{array}{c}\dfrac{(a^{\frac{3}{2}}-a^{-\frac{1}{2}})(\sigma_{zx}^\infty-\mathrm{i}\sigma_{zy}^\infty)}{\xi+\mathrm{i}a^{\frac{1}{2}}}-\dfrac{(a^{\frac{3}{2}}-a^{-\frac{1}{2}})(\sigma_{zx}^\infty+\mathrm{i}\sigma_{zy}^\infty)}{\xi-\mathrm{i}a^{\frac{1}{2}}}\\[3mm]-\dfrac{(a^{\frac{1}{2}}-a^{-\frac{3}{2}})(\sigma_{zx}^\infty+\mathrm{i}\sigma_{zy}^\infty)}{\xi+\mathrm{i}a^{-\frac{1}{2}}}+\dfrac{(a^{\frac{1}{2}}-a^{-\frac{3}{2}})(\sigma_{zx}^\infty-\mathrm{i}\sigma_{zy}^\infty)}{\xi-\mathrm{i}a^{-\frac{1}{2}}}\end{array}\right]$$

$$+\frac{\mu_1\sqrt{(\xi-\mathrm{e}^{\mathrm{i}\psi})(\xi-\mathrm{e}^{-\mathrm{i}\psi})}}{2\mu_2(\mu_1+\mu_2)}\times$$

$$\left[\begin{array}{c}\dfrac{(a^{\frac{3}{2}}-a^{-\frac{1}{2}})(\sigma_{zx}^\infty-\mathrm{i}\sigma_{zy}^\infty)}{\sqrt{(-\mathrm{i}a^{\frac{1}{2}}-\mathrm{e}^{\mathrm{i}\psi})(-\mathrm{i}a^{\frac{1}{2}}-\mathrm{e}^{-\mathrm{i}\psi})}(\xi+\mathrm{i}a^{\frac{1}{2}})}-\dfrac{(a^{\frac{3}{2}}-a^{-\frac{1}{2}})(\sigma_{zx}^\infty+\mathrm{i}\sigma_{zy}^\infty)}{\sqrt{(\mathrm{i}a^{\frac{1}{2}}-\mathrm{e}^{\mathrm{i}\psi})(\mathrm{i}a^{\frac{1}{2}}-\mathrm{e}^{-\mathrm{i}\psi})}(\xi-\mathrm{i}a^{\frac{1}{2}})}+\\[3mm]\dfrac{(a^{\frac{1}{2}}-a^{-\frac{3}{2}})(\sigma_{zx}^\infty+\mathrm{i}\sigma_{zy}^\infty)}{\sqrt{(-\mathrm{i}a^{-\frac{1}{2}}-\mathrm{e}^{\mathrm{i}\psi})(-\mathrm{i}a^{-\frac{1}{2}}-\mathrm{e}^{-\mathrm{i}\psi})}(\xi+\mathrm{i}a^{-\frac{1}{2}})}-\dfrac{(a^{\frac{1}{2}}-a^{-\frac{3}{2}})(\sigma_{zx}^\infty-\mathrm{i}\sigma_{zy}^\infty)}{\sqrt{(\mathrm{i}a^{-\frac{1}{2}}-\mathrm{e}^{\mathrm{i}\psi})(\mathrm{i}a^{-\frac{1}{2}}-\mathrm{e}^{-\mathrm{i}\psi})}(\xi-\mathrm{i}a^{-\frac{1}{2}})}\end{array}\right],$$

$|\xi| \geq 1$ and $\mathrm{Im}\{\xi\} \leq 0$, where the branch cut of the multi-valued function $\sqrt{(\xi - \mathrm{e}^{\mathrm{i}\psi})(\xi - \mathrm{e}^{-\mathrm{i}\psi})}$ is chosen to be along $|\xi| = 1$ and $\psi < \arg(\xi) \leq \pi$, $-\pi \leq \arg(\xi) < -\psi$. It can be easily verified that the obtained analytic functions $f_1(\xi)$ and $f_2(\xi)$ satisfy $\mathrm{Re}\{f_1(\xi)\} = 0$ and $\mathrm{Re}\{f_2(\xi)\} = 0$ on $\mathrm{Im}\{\xi\} = 0$. Thus, all the existing boundary conditions have been satisfied identically.

3. Fracture parameters

Fracture parameters such as stress intensity factors and displacement jumps across the crack surfaces can be extracted from the analytical solution derived in Sec. 2. The mode-III stress intensity factors K_{III}^L, K_{III}^R and K_{III}^D at the three crack tips $z = 1/a$, $z = a$ and $z = \exp(\mathrm{i}\theta_0)$ can be given concisely as

$$(3.1) \qquad K_{\mathrm{III}}^L = \frac{\mu_1}{\mu_1 + \mu_2}\sqrt{\frac{\pi(a^2 - 1)}{2a}}$$

$$\times \left[(a+1)\sigma_{zy}^\infty - \mathrm{Re}\left\{\frac{[a^{\frac{1}{2}}(\cos\psi + a) + \mathrm{i}(a\cos\psi + 1)](\sigma_{zx}^\infty + \mathrm{i}\sigma_{zy}^\infty)}{\sqrt{(\mathrm{i}a^{\frac{1}{2}} - \mathrm{e}^{\mathrm{i}\psi})(\mathrm{i}a^{\frac{1}{2}} - \mathrm{e}^{-\mathrm{i}\psi})}}\right\}\right],$$

$$(3.2) \qquad K_{\mathrm{III}}^R = \frac{\mu_1}{\mu_1 + \mu_2}\sqrt{\frac{\pi(a^2 - 1)}{2a^3}}$$

$$\times \left[\frac{\mu_2}{\mu_1}(a+1)\sigma_{zy}^\infty + \mathrm{Re}\left\{\frac{[a^{\frac{1}{2}}(\cos\psi + a) + \mathrm{i}(a\cos\psi + 1)](\sigma_{zx}^\infty + \mathrm{i}\sigma_{zy}^\infty)}{\sqrt{(\mathrm{i}a^{\frac{1}{2}} - \mathrm{e}^{\mathrm{i}\psi})(\mathrm{i}a^{\frac{1}{2}} - \mathrm{e}^{-\mathrm{i}\psi})}}\right\}\right],$$

$$(3.3) \qquad K_{\text{III}}^D = \frac{\mu_1}{\mu_1 + \mu_2} \sin\frac{\psi}{2} \frac{\sqrt{2\pi(a - a^{-1})\sin\psi}}{a^2 + 1 + 2a\cos 2\psi}$$

$$\times \operatorname{Re}\left\{ (\mathrm{i}a^{\frac{1}{2}} - \mathrm{e}^{\mathrm{i}\psi})^{\frac{3}{2}} (\mathrm{i}a^{\frac{1}{2}} - \mathrm{e}^{-\mathrm{i}\psi})^{\frac{3}{2}} (\mathrm{i}a^{\frac{1}{2}} - 1)(\sigma_{zy}^\infty + \mathrm{i}\sigma_{zx}^\infty) \right\}.$$

It is observed from Eqs. (3.1) and (3.2) that

$$(3.4) \qquad\qquad K_{\text{III}}^L + aK_{\text{III}}^R = \sigma_{zy}^\infty \sqrt{\frac{\pi(a-1)(a+1)^3}{2a}},$$

which indicates that the sum $(K_{\text{III}}^L + aK_{\text{III}}^R)$ is independent of the remote stress component σ_{zx}^∞, the shear moduli μ_1, μ_2, and the length of the arc crack L_c.

The displacement jumps across the two surfaces of the radial matrix crack and across those of the arc interface crack L_c can be finally derived as

$$(3.5) \qquad \Delta w_1(u) = -\frac{2(a+1)(a^{\frac{3}{2}} - a^{-\frac{1}{2}})}{\mu_1 + \mu_2} \frac{u(u^2+1)\sigma_{zy}^\infty}{(u^2+a)(au^2+1)}$$

$$+ \frac{a^2-1}{\mu_1 + \mu_2} u \left[\sqrt{u^2 + 1 + 2u\cos\psi} + \sqrt{u^2 + 1 - 2u\cos\psi} \right]$$

$$\times \left(\frac{\operatorname{Re}\left\{ \frac{\sigma_{zx}^\infty + \mathrm{i}\sigma_{zy}^\infty}{\sqrt{(\mathrm{i}a^{\frac{1}{2}} - \mathrm{e}^{\mathrm{i}\psi})(\mathrm{i}a^{\frac{1}{2}} - \mathrm{e}^{-\mathrm{i}\psi})}} \right\}}{au^2+1} - \frac{\operatorname{Im}\left\{ \frac{\sigma_{zx}^\infty + \mathrm{i}\sigma_{zy}^\infty}{\sqrt{(\mathrm{i}a^{\frac{1}{2}} - \mathrm{e}^{\mathrm{i}\psi})(\mathrm{i}a^{\frac{1}{2}} - \mathrm{e}^{-\mathrm{i}\psi})}} \right\}}{a^{\frac{1}{2}}(u^2+a)} \right)$$

$$+ \frac{a^2-1}{\mu_1 + \mu_2} \left[\sqrt{u^2 + 1 + 2u\cos\psi} - \sqrt{u^2 + 1 - 2u\cos\psi} \right]$$

$$\times \left(\frac{\operatorname{Re}\left\{ \frac{\sigma_{zx}^\infty + \mathrm{i}\sigma_{zy}^\infty}{\sqrt{(\mathrm{i}a^{\frac{1}{2}} - \mathrm{e}^{\mathrm{i}\psi})(\mathrm{i}a^{\frac{1}{2}} - \mathrm{e}^{-\mathrm{i}\psi})}} \right\}}{u^2+a} - \frac{\operatorname{Im}\left\{ \frac{\sigma_{zx}^\infty + \mathrm{i}\sigma_{zy}^\infty}{\sqrt{(\mathrm{i}a^{\frac{1}{2}} - \mathrm{e}^{\mathrm{i}\psi})(\mathrm{i}a^{\frac{1}{2}} - \mathrm{e}^{-\mathrm{i}\psi})}} \right\}}{a^{\frac{1}{2}}(au^2+1)} \right),$$

$$(-1 \leq u \leq 0);$$

$$(3.6) \qquad \Delta w_2(u) = -\frac{2(a+1)(a^{\frac{3}{2}} - a^{-\frac{1}{2}})}{\mu_1 + \mu_2} \frac{u(u^2+1)\sigma_{zy}^\infty}{(u^2+a)(au^2+1)}$$

$$+ \frac{\mu_1(a^2-1)}{\mu_2(\mu_1 + \mu_2)} \left[\sqrt{u^2 + 1 + 2u\cos\psi} + \sqrt{u^2 + 1 - 2u\cos\psi} \right]$$

$$\times \left(\frac{\operatorname{Re}\left\{ \frac{\sigma_{zx}^\infty + \mathrm{i}\sigma_{zy}^\infty}{\sqrt{(\mathrm{i}a^{\frac{1}{2}} - \mathrm{e}^{\mathrm{i}\psi})(\mathrm{i}a^{\frac{1}{2}} - \mathrm{e}^{-\mathrm{i}\psi})}} \right\}}{u^2+a} - \frac{\operatorname{Im}\left\{ \frac{\sigma_{zx}^\infty + \mathrm{i}\sigma_{zy}^\infty}{\sqrt{(\mathrm{i}a^{\frac{1}{2}} - \mathrm{e}^{\mathrm{i}\psi})(\mathrm{i}a^{\frac{1}{2}} - \mathrm{e}^{-\mathrm{i}\psi})}} \right\}}{a^{\frac{1}{2}}(au^2+1)} \right)$$

$$+ \frac{\mu_1(a^2-1)}{\mu_2(\mu_1+\mu_2)} u \left[\sqrt{u^2+1+2u\cos\psi} - \sqrt{u^2+1-2u\cos\psi} \right]$$

$$\times \left(\frac{\mathrm{Re}\left\{ \frac{\sigma_{zx}^\infty + \mathrm{i}\sigma_{zy}^\infty}{\sqrt{(\mathrm{i}a^{\frac{1}{2}}-\mathrm{e}^{\mathrm{i}\psi})(\mathrm{i}a^{\frac{1}{2}}-\mathrm{e}^{-\mathrm{i}\psi})}} \right\}}{au^2+1} - \frac{\mathrm{Im}\left\{ \frac{\sigma_{zx}^\infty + \mathrm{i}\sigma_{zy}^\infty}{\sqrt{(\mathrm{i}a^{\frac{1}{2}}-\mathrm{e}^{\mathrm{i}\psi})(\mathrm{i}a^{\frac{1}{2}}-\mathrm{e}^{-\mathrm{i}\psi})}} \right\}}{a^{\frac{1}{2}}(u^2+a)} \right),$$

$$(u \le -1);$$

$$(3.7) \qquad w_2 - w_1 = \frac{a^{\frac{3}{2}} - a^{-\frac{1}{2}}}{\mu_2}$$

$$\times \mathrm{Im}\left\{ \frac{\sqrt{(\xi - \mathrm{e}^{\mathrm{i}\psi})(\xi - \mathrm{e}^{-\mathrm{i}\psi})}}{\sqrt{(\mathrm{i}a^{\frac{1}{2}} - \mathrm{e}^{\mathrm{i}\psi})(\mathrm{i}a^{\frac{1}{2}} - \mathrm{e}^{-\mathrm{i}\psi})}} \left(\frac{1}{\xi - \mathrm{i}a^{\frac{1}{2}}} - \frac{1}{1 - \mathrm{i}a^{\frac{1}{2}}\xi} \right) (\sigma_{zx}^\infty + \mathrm{i}\sigma_{zy}^\infty) \right\},$$

$$(|\xi| = 1 \text{ and } -\pi \le \arg(\xi) \le -\psi),$$

where $\sqrt{(\xi - \mathrm{e}^{\mathrm{i}\psi})(\xi - \mathrm{e}^{-\mathrm{i}\psi})}$ is chosen to be the branch by approaching L_c from inside the interface.

4. Discussions and numerical result

In this section we will first present some special cases to verify and to demonstrate the obtained analytic solution. Then numerical result will be presented to visually illustrate the influence of the length of the arc crack L_c (characterized by θ_0) and that of the radial matrix crack (characterized by $a > 1$) on the variations of the stress intensity factors at the three crack tips, and on the displacement jumps across the crack surfaces.

4.1. Discussions

(i) $\psi = \pi$ (*or equivalently* $\theta_0 = 0$). In this case the crack penetrates a perfectly bonded inhomogeneity. By letting $\psi = \pi$ (or equivalently $\theta_0 = 0$), Eqs. (3.1) and (3.2) become

$$K_{\mathrm{III}}^L = \frac{2\mu_1}{\mu_1+\mu_2} \sqrt{\frac{\pi(a - a^{-1})}{2}} \sigma_{zy}^\infty,$$

$$K_{\mathrm{III}}^R = \sqrt{\frac{\pi(a - a^{-1})}{2}} \left(1 + \frac{\mu_2 - \mu_1}{\mu_1+\mu_2} a^{-1} \right) \sigma_{zy}^\infty,$$

which just recovers the result in [14]. In this case we have $K_{\mathrm{III}}^D = 0$.

(ii) $\psi = \pi/2$ (*or equivalently* $\theta_0 = \pi$). In this case the upper half circular interface is debonded. By letting $\psi = \pi/2$ (or equivalently $\theta_0 = \pi$), Eqs. (3.1) and (3.2) become

$$K^L_{\text{III}} = \frac{\mu_1}{\mu_1 + \mu_2} \sqrt{\frac{\pi(a^2 - 1)}{2a}} \left[\left(a + 1 - \frac{a^{\frac{3}{2}}}{\sqrt{a-1}} \right) \sigma^\infty_{zy} - \frac{\sigma^\infty_{zx}}{\sqrt{a-1}} \right],$$

$$K^R_{\text{III}} = \frac{\mu_1}{\mu_1 + \mu_2} \sqrt{\frac{\pi(a^2 - 1)}{2a^3}} \left[\left(\frac{\mu_2}{\mu_1}(a + 1) + \frac{a^{\frac{3}{2}}}{\sqrt{a-1}} \right) \sigma^\infty_{zy} + \frac{\sigma^\infty_{zx}}{\sqrt{a-1}} \right],$$

$$K^D_{\text{III}} = \frac{\mu_1}{\mu_1 + \mu_2} \sqrt{\frac{\pi(a + 1)}{a}} (a^{\frac{1}{2}}\sigma^\infty_{zy} - \sigma^\infty_{zx}).$$

(iii) $\psi = 0$ (*or equivalently* $\theta_0 = 2\pi$). In this case the entire circular interface is debonded. By letting $\psi = 0$ (or equivalently $\theta_0 = 2\pi$), Eqs. (3.1)–(3.3) become

$$K^L_{\text{III}} = K^D_{\text{III}} = 0,$$

(4.1)
$$K^R_{\text{III}} = \sqrt{\frac{\pi(a - a^{-1})}{2}}(1 + a^{-1})\sigma^\infty_{zy}.$$

In addition Eq. (4.1) can also be obtained by allowing $\mu_1 = 0$ in Eq. (3.2).

(iv) $\theta_0 \to 0$. In this case the length of the arc crack L_c is very small, and Eq. (3.3) becomes

$$K^D_{\text{III}} \approx \frac{\mu_1}{\mu_1 + \mu_2} \sqrt{\frac{\pi\theta_0}{a}} \left[(a - 1)\sigma^\infty_{zy} + 2a^{\frac{1}{2}}\sigma^\infty_{zx} \right].$$

(v) $a \to \infty$. In this case the matrix crack becomes semi-infinite, and the remote field is controlled by K^∞_{III}. Now Eqs. (3.1) and (3.3) become

(4.2)
$$K^L_{\text{III}} = \frac{\mu_1}{\mu_1 + \mu_2} \left(1 + \cos\frac{\theta_0}{2} \right) K^\infty_{\text{III}},$$

(4.3)
$$K^D_{\text{III}} = \frac{2\mu_1}{\mu_1 + \mu_2} \cos\frac{\theta_0}{4} \sqrt{\sin\frac{\theta_0}{2}} K^\infty_{\text{III}}.$$

It is observed from Eqs. (4.2) and (4.3) that:

(i) K^L_{III} is a decreasing function of θ_0, $(0 \leq \theta_0 \leq 2\pi)$: $K^L_{\text{III}} = \frac{2\mu_1}{\mu_1 + \mu_2}K^\infty_{\text{III}}$ when $\theta_0 = 0$ and $K^L_{\text{III}} = 0$ when $\theta_0 = 2\pi$;

(ii) K^D_{III} attains its maximum value of $K^D_{\text{III}} = \frac{(\frac{27}{4})^{1/4}\mu_1}{\mu_1 + \mu_2}K^\infty_{\text{III}} \approx \frac{1.6119\mu_1}{\mu_1 + \mu_2}K^\infty_{\text{III}}$ when $\theta_0 = 2\pi/3$.

4.2. Numerical result

We illustrate in Figs. 3–6 the variations of K_{III}^{L} and K_{III}^{D} for different values of the parameters a and θ_0. Once K_{III}^{L} is known, K_{III}^{R} can be obtained by using the identity (3.4). It is observed from Figs. 3 and 4 that when the matrix is
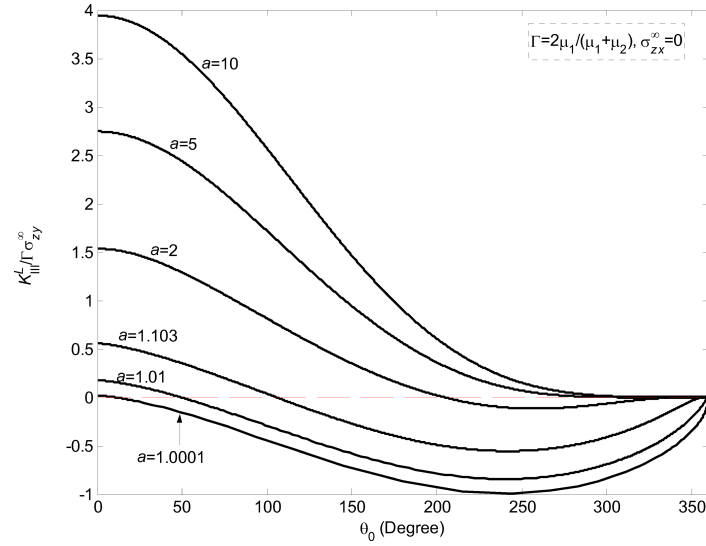
Fig. 3. The variations of K_{III}^{L} for different values of the parameters a and θ_0 when the matrix is only subjected to σ_{zy}^{∞}.
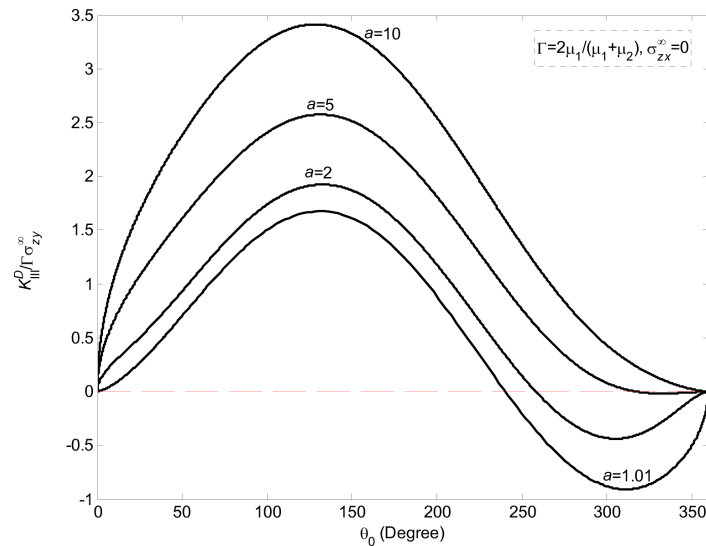
Fig. 4. The variations of K_{III}^{D} for different values of the parameters a and θ_0 when the matrix is only subjected to σ_{zy}^{∞}.
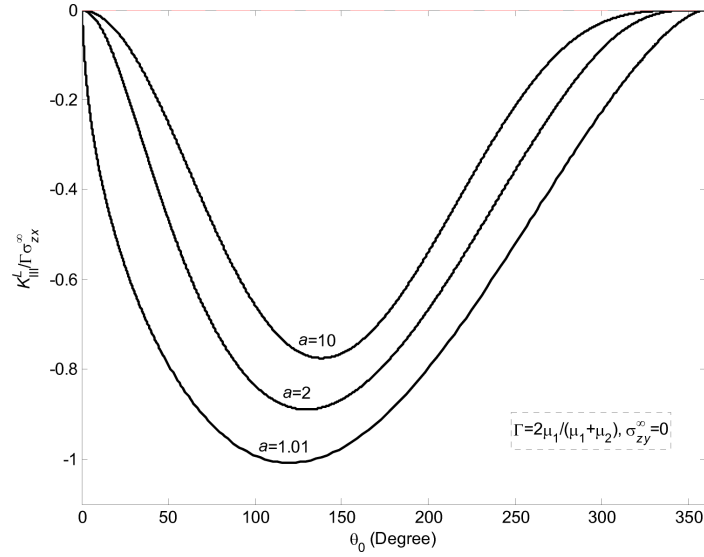
FIG. 5. The variations of K_{III}^{L} for different values of the parameters a and θ_0 when the matrix is only subjected to σ_{zx}^{∞}.
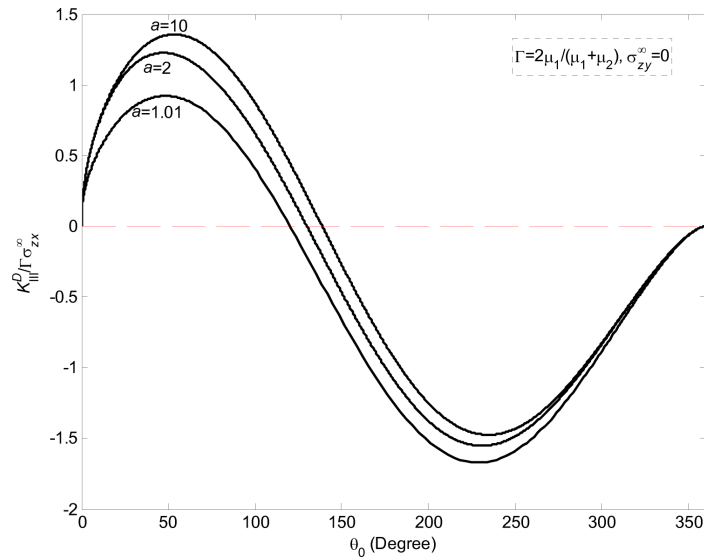
FIG. 6. The variations of K_{III}^{D} for different values of the parameters a and θ_0 when the matrix is only subjected to σ_{zx}^{∞}.

subjected to only σ_{zy}^{∞} (with $\sigma_{zx}^{\infty} = 0$), (i) K_{III}^{L} attains its maximum absolute value at $\theta_0 = 0$ if $a \geq 1.103$ or at $\theta_0 \approx 240°$ if $a < 1.103$, K_{III}^{D} always attains its maximum absolute value at $\theta_0 \approx 129°$ for a fixed value of a; (ii) interestingly

as $a \to 1$, K_{III}^L attains its maximum absolute value of $\Gamma|\sigma_{zy}^\infty|$; (iii) K_{III}^L (or K_{III}^D) can be zero at a certain value of $\theta_0 < 360°$. It is observed from Figs. 5 and 6 that when the matrix is subjected to only σ_{zx}^∞ (with $\sigma_{zy}^\infty = 0$), (i) K_{III}^L (or K_{III}^D) attains its maximum absolute value at a certain value of $\theta_0 < 360°$ for a fixed value of a; (ii) K_{III}^L and σ_{zx}^∞ always have opposite signs, whilst K_{III}^D can be zero at a certain value of $\theta_0 < 150°$.

We show in Figs. 7–10 the displacement jumps across the two surfaces of the radial matrix crack and across those of the arc interface crack for different values of θ_0 with $\mu_1 = 3\mu_2$ and $a = 2$. It is observed from Figs. 7 and 8 for the loading case when the matrix is only subjected to $\sigma_{zy}^\infty > 0$ that:

(i) in the absence of the circular crack L_c when $\theta_0 = 0$, the obtained displacement jump $w(x, 0^+) - w(x, 0^-)$ coincides with that reported in [14];

(ii) when the entire circular interface is debonded (i.e., $\theta_0 = 360°$), $w_2(x, 0^+) - w_2(x, 0^-)$ in the matrix is also in agreement with [14];

(iii) as θ_0 increases from zero to 258°, the value of $w_2(x, 0^+) - w_2(x, 0^-)$ at a fixed point x in the matrix monotonically increases, whilst that of $w_1(x, 0^+) - w_1(x, 0^-)$ at a fixed point x in the inhomogeneity monotonically decreases;

(iv) as θ_0 increases from 258° to 360°, the value of $w_2(x, 0^+) - w_2(x, 0^-)$ at a fixed point x in the matrix monotonically decreases, whilst that of $w_1(x, 0^+) - w_1(x, 0^-)$ at a fixed point x in the inhomogeneity monotonically increases;
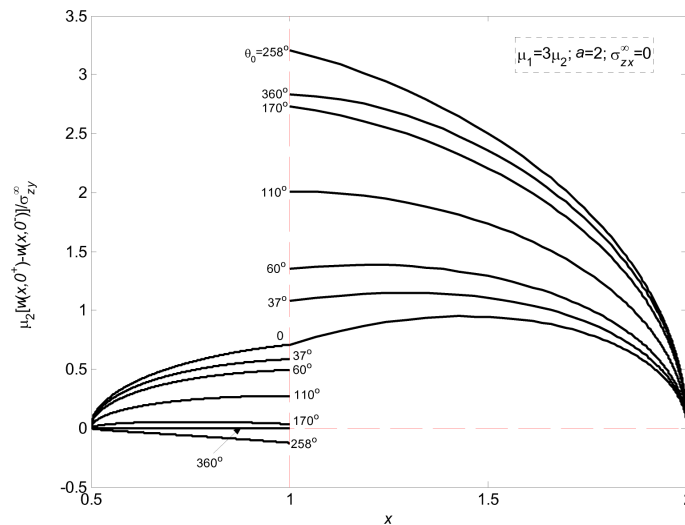
FIG. 7. The displacement jump $w(x, 0^+) - w(x, 0^-)$ across the two surfaces of the radial matrix crack for different values of θ_0 with $\mu_1 = 3\mu_2$ and $a = 2$ when the matrix is only subjected to $\sigma_{zy}^\infty > 0$.

(v) for a certain value of θ_0, $(w_2 - w_1)$ at $\theta = 0$ (see Fig. 8) is exactly the same as the difference in displacement jump across the debonded interface: $[w_2(1, 0^+) - w_2(1, 0^-)] - [w_1(1, 0^+) - w_1(1, 0^-)]$ (see Fig. 7);

(vi) when $\theta_0 \leq 258°$, $(w_2 - w_1)$ is always positive;

(vii) when $258° < \theta_0 \leq 360°$, $(w_2 - w_1)$ can be positive as well as negative.
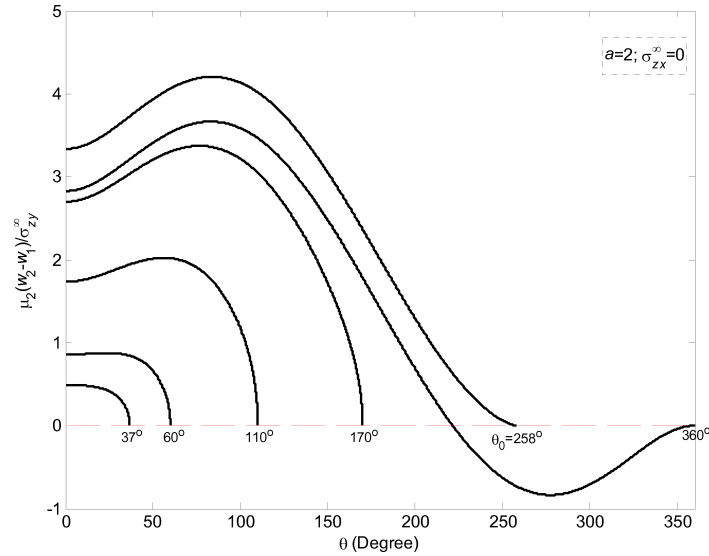
FIG. 8. The displacement jump $(w_2 - w_1)$ across the two surfaces of the arc crack L_c for different values of θ_0 with $a = 2$ when the matrix is only subjected to $\sigma_{zy}^\infty > 0$.

It is observed from Figs. 9 and 10 for the loading case when the matrix is subjected to only $\sigma_{zx}^\infty > 0$ that:

(i) as θ_0 increases from zero to $130°$, the absolute value of $w(x, 0^+) - w(x, 0^-)$ at a fixed point x either in the matrix or in the inhomogeneity monotonically increases;

(ii) as θ_0 increases from $130°$ to $360°$, the absolute value of $w(x, 0^+) - w(x, 0^-)$ at a fixed point x either in the matrix or in the inhomogeneity monotonically decreases;

(iii) for a certain value of θ_0, $(w_2 - w_1)$ at $\theta = 0$ (see Fig. 10) is exactly the same as the difference in displacement jump across the debonded interface: $[w_2(1, 0^+) - w_2(1, 0^-)] - [w_1(1, 0^+) - w_1(1, 0^-)]$ (see Fig. 9);

(iv) when $\theta_0 \leq 130°$, the jump $(w_2 - w_1)$ is always positive;

(v) when $130° < \theta_0 < 360°$, the jump $(w_2 - w_1)$ can be positive as well as negative;

(vi) when $\theta_0 = 360°$, the jump $(w_2 - w_1)$ can only be negative.
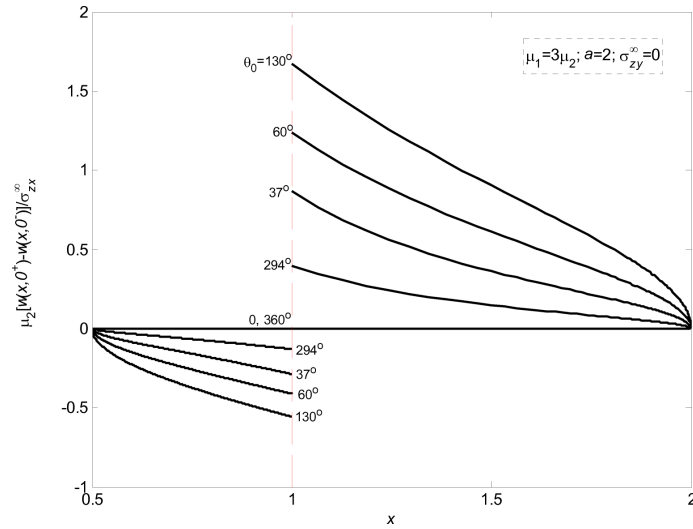
FIG. 9. The displacement jump $w(x, 0^+) - w(x, 0^-)$ across the two surfaces of the radial matrix crack for different values of θ_0 with $\mu_1 = 3\mu_2$ and $a = 2$ when the matrix is only subjected to $\sigma_{zx}^\infty > 0$.
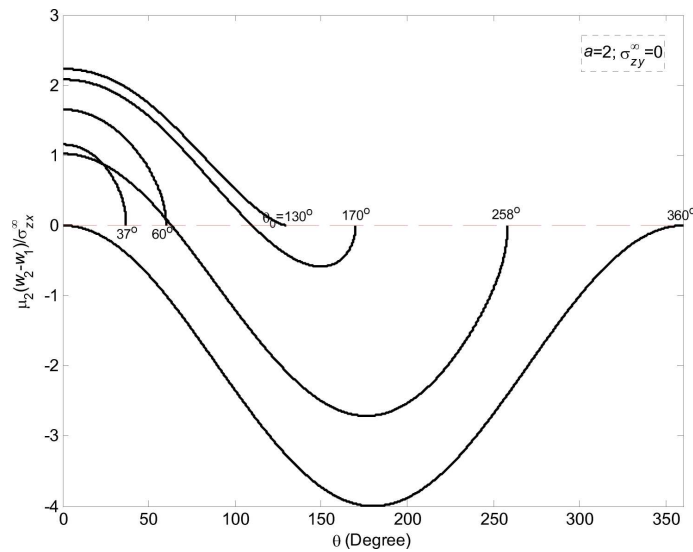
FIG. 10. The displacement jump $(w_2 - w_1)$ across the two surfaces of the arc crack L_c for different values of θ_0 with $a = 2$ when the matrix is only subjected to $\sigma_{zx}^\infty > 0$.

5. Other loadings

In the above analysis, we have assumed that the displacement is single-valued for any contour surrounding the radial crack and the circular interface crack

L_c and that the matrix is subjected to only remote uniform stresses. In the following three subsections, we consider the three loading cases: (i) the radial crack and the arc interface crack form a Zener–Stroh crack [10, 16]; (ii) a screw dislocation is located in the matrix; and (iii) a screw dislocation is located in the inhomogeneity. For loading cases (ii) and (iii), the radial crack and the arc interface crack form a Griffith crack.

5.1. A Zener–Stroh crack

We consider the loading case in which the radial crack and the arc crack form a Zener–Stroh crack. In addition we assume that the sum of the Burgers vector inside the Zener–Stroh crack is b. The two analytic functions $f_1'(\xi)$ and $f_2'(\xi)$ for this loading case can be derived as

$$
f_1'(\xi) = -\frac{\mu_2 b}{2\pi(\mu_1 + \mu_2)}\left[\frac{1}{\xi + ia^{\frac{1}{2}}} - \frac{1}{\xi - ia^{\frac{1}{2}}} - \frac{1}{\xi + ia^{-\frac{1}{2}}} + \frac{1}{\xi - ia^{-\frac{1}{2}}}\right]
$$

$$
-\frac{\mu_2 b}{2\pi(\mu_1 + \mu_2)\sqrt{(\xi - e^{i\psi})(\xi - e^{-i\psi})}}
$$

$$
\times \left[\begin{array}{l}
\dfrac{\sqrt{(-ia^{\frac{1}{2}} - e^{i\psi})(-ia^{\frac{1}{2}} - e^{-i\psi})}}{\xi + ia^{\frac{1}{2}}} - \dfrac{\sqrt{(ia^{\frac{1}{2}} - e^{i\psi})(ia^{\frac{1}{2}} - e^{-i\psi})}}{\xi - ia^{\frac{1}{2}}} \\[4mm]
+\dfrac{\sqrt{(-ia^{-\frac{1}{2}} - e^{i\psi})(-ia^{-\frac{1}{2}} - e^{-i\psi})}}{\xi + ia^{-\frac{1}{2}}} - \dfrac{\sqrt{(ia^{-\frac{1}{2}} - e^{i\psi})(ia^{-\frac{1}{2}} - e^{-i\psi})}}{\xi - ia^{-\frac{1}{2}}}
\end{array}\right],
$$

$|\xi| \leq 1$ and $\mathrm{Im}\{\xi\} \leq 0$;

$$
f_2'(\xi) = -\frac{\mu_2 b}{2\pi(\mu_1 + \mu_2)}\left[\frac{1}{\xi + ia^{\frac{1}{2}}} - \frac{1}{\xi - ia^{\frac{1}{2}}} - \frac{1}{\xi + ia^{-\frac{1}{2}}} + \frac{1}{\xi - ia^{-\frac{1}{2}}}\right]
$$

$$
-\frac{\mu_1 b}{2\pi(\mu_1 + \mu_2)\sqrt{(\xi - e^{i\psi})(\xi - e^{-i\psi})}}
$$

$$
\times \left[\begin{array}{l}
\dfrac{\sqrt{(-ia^{\frac{1}{2}} - e^{i\psi})(-ia^{\frac{1}{2}} - e^{-i\psi})}}{\xi + ia^{\frac{1}{2}}} - \dfrac{\sqrt{(ia^{\frac{1}{2}} - e^{i\psi})(ia^{\frac{1}{2}} - e^{-i\psi})}}{\xi - ia^{\frac{1}{2}}} \\[4mm]
+\dfrac{\sqrt{(-ia^{-\frac{1}{2}} - e^{i\psi})(-ia^{-\frac{1}{2}} - e^{-i\psi})}}{\xi + ia^{-\frac{1}{2}}} - \dfrac{\sqrt{(ia^{-\frac{1}{2}} - e^{i\psi})(ia^{-\frac{1}{2}} - e^{-i\psi})}}{\xi - ia^{-\frac{1}{2}}}
\end{array}\right],
$$

$|\xi| \geq 1$ and $\mathrm{Im}\{\xi\} \leq 0$.

REMARK. For the three loading cases discussed above and the following in this section, we can derive only closed-form expressions of $f_1'(\xi)$ and $f_2'(\xi)$, i.e., elementary expressions of $f_1(\xi)$ and $f_2(\xi)$ cannot be obtained for these loading cases.

Once the two analytic functions have been derived, the mode-III stress intensity factors K_{III}^L, K_{III}^R and K_{III}^D at the three crack tips $z = 1/a$, $z = a$ and $z = \exp(\mathrm{i}\theta_0)$ can be concisely given by

$$(5.1) \quad K_{\text{III}}^L = \frac{\mu_1\mu_2 b}{\mu_1 + \mu_2} \sqrt{\frac{a}{2\pi(a^2 - 1)}}$$
$$\times \left[a - 1 - \mathrm{Re}\left\{ (1 - \mathrm{i}a^{\frac{1}{2}})\sqrt{(\mathrm{i}a^{\frac{1}{2}} - \mathrm{e}^{\mathrm{i}\psi})(\mathrm{i}a^{\frac{1}{2}} - \mathrm{e}^{-\mathrm{i}\psi})} \right\} \right],$$

$$(5.2) \quad K_{\text{III}}^R = \frac{\mu_1\mu_2 b}{\mu_1 + \mu_2} \frac{1}{\sqrt{2\pi(a^3 - a)}}$$
$$\times \left[\frac{\mu_2}{\mu_1}(a - 1) + \mathrm{Re}\left\{ (1 - \mathrm{i}a^{\frac{1}{2}})\sqrt{(\mathrm{i}a^{\frac{1}{2}} - \mathrm{e}^{\mathrm{i}\psi})(\mathrm{i}a^{\frac{1}{2}} - \mathrm{e}^{-\mathrm{i}\psi})} \right\} \right],$$

$$(5.3) \quad K_{\text{III}}^D = \frac{\mu_1\mu_2 b}{\mu_1 + \mu_2} \sqrt{\frac{a^2 + 1 + 2a\cos 2\psi}{\pi(a^2 - 1)\tan\frac{\psi}{2}}} \, \mathrm{Im}\left\{ \frac{1 - \mathrm{i}a^{\frac{1}{2}}}{\sqrt{(\mathrm{i}a^{\frac{1}{2}} - \mathrm{e}^{\mathrm{i}\psi})(\mathrm{i}a^{\frac{1}{2}} - \mathrm{e}^{-\mathrm{i}\psi})}} \right\},$$

from which the following identity can be arrived at

$$(5.4) \quad K_{\text{III}}^L + aK_{\text{III}}^R = \mu_2 b \sqrt{\frac{a(a - 1)}{2\pi(a + 1)}}.$$

The above identity indicates that the sum $(K_{\text{III}}^L + aK_{\text{III}}^R)$ is independent of the shear modulus μ_1 of the inhomogeneity, and the length of the arc crack L_c.

When $\psi = \pi$ (or equivalently $\theta_0 = 0$) for a Zener–Stroh crack penetrating a perfectly bonded circular inhomogeneity, Eqs. (5.1) and (5.2) become

$$K_{\text{III}}^L = -\frac{2\mu_1\mu_2 b}{(\mu_1 + \mu_2)\sqrt{2\pi(a - a^{-1})}},$$

$$K_{\text{III}}^R = \frac{\mu_2 b}{\sqrt{2\pi(a - a^{-1})}}\left[1 + a^{-1}\frac{\mu_1 - \mu_2}{\mu_1 + \mu_2} \right],$$

which again recovers the result in [14].

Figures 11 and 12 illustrate the variations of K_{III}^L and K_{III}^D for different values of the parameters a and θ_0 of the Zener–Stroh crack. It is observed from the two figures that: (i) $K_{\text{III}}^L b < 0$, $K_{\text{III}}^D b < 0$; (ii) For a fixed value of θ_0, the

magnitudes of both K_{III}^L and K_{III}^D decrease as a increases. It is observed from Fig. 11 that $|K_{III}^L|$ is a decreasing function of θ_0 for a fixed value of a: $(K_{III}^L)_{\theta_0=0} = -\Gamma\mu_2 b/\sqrt{2\pi(a-a^{-1})}$ with $\Gamma = 2\mu_1/(\mu_1 + \mu_2)$ and $(K_{III}^L)_{\theta_0=360°} = 0$. Also, from Fig. 12, K_{III}^D attains its maximum absolute value at a certain value of
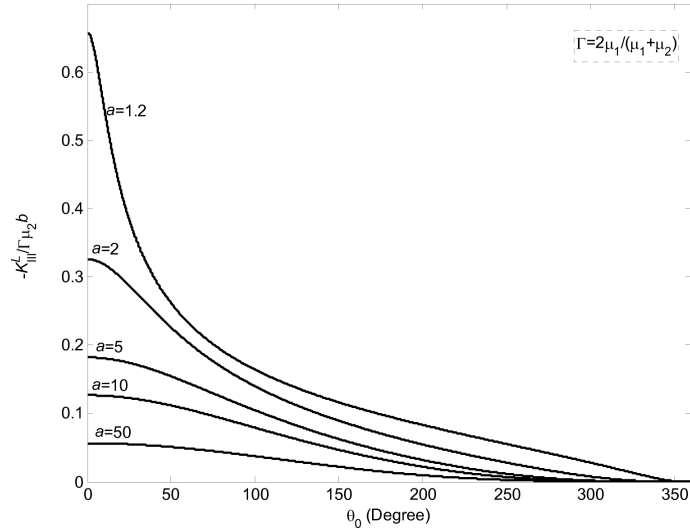
FIG. 11. The variations of K_{III}^L for different values of the parameters a and θ_0 of the Zener–Stroh crack.
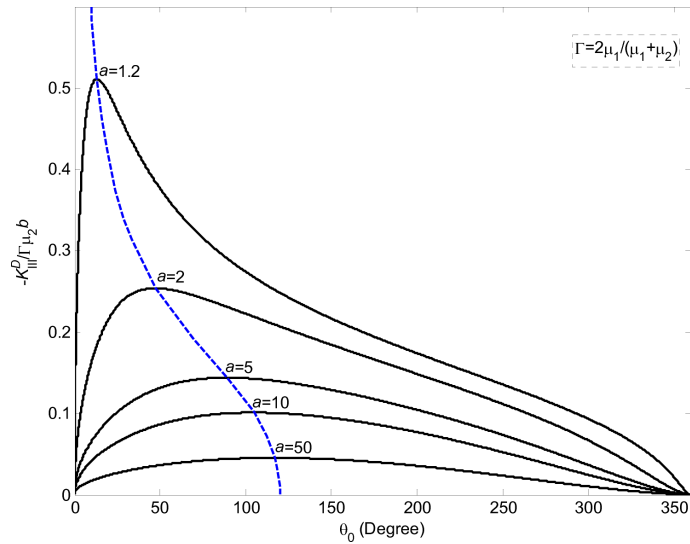
FIG. 12. The variations of K_{III}^D for different values of the parameters a and θ_0 of the Zener–Stroh crack.

$\theta_0 < 120°$ for a fixed value of a. As a increases, the value of θ_0 at which K_{III}^D attains its maximum absolute value monotonically increases.

5.2. A screw dislocation in the matrix

Next we consider a screw dislocation with Burgers vector b located at $z = z_0$, $(|z_0| > 1)$ in the matrix (or $\xi = \xi_0 = -\sqrt{(1-az_0)/(z_0-a)}$, $(|\xi_0| > 1)$ in the ξ-plane). The two analytic functions $f_1'(\xi)$ and $f_2'(\xi)$ for this loading case can be derived as

$$f_1'(\xi) = \frac{\mu_2 b}{2\pi(\mu_1+\mu_2)}$$

$$\times \left[\frac{1}{\xi-\xi_0} - \frac{1}{\xi-\bar{\xi}_0} - \frac{1}{\xi-\bar{\xi}_0^{-1}} + \frac{1}{\xi-\xi_0^{-1}} - \frac{1}{\xi+\mathrm{i}a^{\frac{1}{2}}} + \frac{1}{\xi-\mathrm{i}a^{\frac{1}{2}}} + \frac{1}{\xi+\mathrm{i}a^{-\frac{1}{2}}} - \frac{1}{\xi-\mathrm{i}a^{-\frac{1}{2}}} \right]$$

$$+ \frac{\mu_2 b}{2\pi(\mu_1+\mu_2)\sqrt{(\xi-\mathrm{e}^{\mathrm{i}\psi})(\xi-\mathrm{e}^{-\mathrm{i}\psi})}}$$

$$\times \begin{bmatrix} \dfrac{\sqrt{(\xi_0-\mathrm{e}^{\mathrm{i}\psi})(\xi_0-\mathrm{e}^{-\mathrm{i}\psi})}}{\xi-\xi_0} - \dfrac{\sqrt{(\bar{\xi}_0-\mathrm{e}^{\mathrm{i}\psi})(\bar{\xi}_0-\mathrm{e}^{-\mathrm{i}\psi})}}{\xi-\bar{\xi}_0} \\[2ex] + \dfrac{\sqrt{(\bar{\xi}_0^{-1}-\mathrm{e}^{\mathrm{i}\psi})(\bar{\xi}_0^{-1}-\mathrm{e}^{-\mathrm{i}\psi})}}{\xi-\bar{\xi}_0^{-1}} - \dfrac{\sqrt{(\xi_0^{-1}-\mathrm{e}^{\mathrm{i}\psi})(\xi_0^{-1}-\mathrm{e}^{-\mathrm{i}\psi})}}{\xi-\xi_0^{-1}} \\[2ex] - \dfrac{\sqrt{(-\mathrm{i}a^{\frac{1}{2}}-\mathrm{e}^{\mathrm{i}\psi})(-\mathrm{i}a^{\frac{1}{2}}-\mathrm{e}^{-\mathrm{i}\psi})}}{\xi+\mathrm{i}a^{\frac{1}{2}}} + \dfrac{\sqrt{(\mathrm{i}a^{\frac{1}{2}}-\mathrm{e}^{\mathrm{i}\psi})(\mathrm{i}a^{\frac{1}{2}}-\mathrm{e}^{-\mathrm{i}\psi})}}{\xi-\mathrm{i}a^{\frac{1}{2}}} \\[2ex] - \dfrac{\sqrt{(-\mathrm{i}a^{-\frac{1}{2}}-\mathrm{e}^{\mathrm{i}\psi})(-\mathrm{i}a^{-\frac{1}{2}}-\mathrm{e}^{-\mathrm{i}\psi})}}{\xi+\mathrm{i}a^{-\frac{1}{2}}} + \dfrac{\sqrt{(\mathrm{i}a^{-\frac{1}{2}}-\mathrm{e}^{\mathrm{i}\psi})(\mathrm{i}a^{-\frac{1}{2}}-\mathrm{e}^{-\mathrm{i}\psi})}}{\xi-\mathrm{i}a^{-\frac{1}{2}}} \end{bmatrix},$$

$|\xi| \leq 1$ and $\mathrm{Im}\{\xi\} \leq 0$,

$$f_2'(\xi) = \frac{\mu_2 b}{2\pi(\mu_1+\mu_2)}$$

$$\times \left[\frac{1}{\xi-\xi_0} - \frac{1}{\xi-\bar{\xi}_0} - \frac{1}{\xi-\bar{\xi}_0^{-1}} + \frac{1}{\xi-\xi_0^{-1}} - \frac{1}{\xi+\mathrm{i}a^{\frac{1}{2}}} + \frac{1}{\xi-\mathrm{i}a^{\frac{1}{2}}} + \frac{1}{\xi+\mathrm{i}a^{-\frac{1}{2}}} - \frac{1}{\xi-\mathrm{i}a^{-\frac{1}{2}}} \right]$$

$$+ \frac{\mu_1 b}{2\pi(\mu_1+\mu_2)\sqrt{(\xi-\mathrm{e}^{\mathrm{i}\psi})(\xi-\mathrm{e}^{-\mathrm{i}\psi})}}$$

$$\times \begin{bmatrix} \dfrac{\sqrt{(\xi_0-\mathrm{e}^{\mathrm{i}\psi})(\xi_0-\mathrm{e}^{-\mathrm{i}\psi})}}{\xi-\xi_0} - \dfrac{\sqrt{(\bar{\xi}_0-\mathrm{e}^{\mathrm{i}\psi})(\bar{\xi}_0-\mathrm{e}^{-\mathrm{i}\psi})}}{\xi-\bar{\xi}_0} \\[2em] + \dfrac{\sqrt{(\bar{\xi}_0^{-1}-\mathrm{e}^{\mathrm{i}\psi})(\bar{\xi}_0^{-1}-\mathrm{e}^{-\mathrm{i}\psi})}}{\xi-\bar{\xi}_0^{-1}} - \dfrac{\sqrt{(\xi_0^{-1}-\mathrm{e}^{\mathrm{i}\psi})(\xi_0^{-1}-\mathrm{e}^{-\mathrm{i}\psi})}}{\xi-\xi_0^{-1}} \\[2em] - \dfrac{\sqrt{(-\mathrm{i}a^{\frac{1}{2}}-\mathrm{e}^{\mathrm{i}\psi})(-\mathrm{i}a^{\frac{1}{2}}-\mathrm{e}^{-\mathrm{i}\psi})}}{\xi+\mathrm{i}a^{\frac{1}{2}}} + \dfrac{\sqrt{(\mathrm{i}a^{\frac{1}{2}}-\mathrm{e}^{\mathrm{i}\psi})(\mathrm{i}a^{\frac{1}{2}}-\mathrm{e}^{-\mathrm{i}\psi})}}{\xi-\mathrm{i}a^{\frac{1}{2}}} \\[2em] - \dfrac{\sqrt{(-\mathrm{i}a^{-\frac{1}{2}}-\mathrm{e}^{\mathrm{i}\psi})(-\mathrm{i}a^{-\frac{1}{2}}-\mathrm{e}^{-\mathrm{i}\psi})}}{\xi+\mathrm{i}a^{-\frac{1}{2}}} + \dfrac{\sqrt{(\mathrm{i}a^{-\frac{1}{2}}-\mathrm{e}^{\mathrm{i}\psi})(\mathrm{i}a^{-\frac{1}{2}}-\mathrm{e}^{-\mathrm{i}\psi})}}{\xi-\mathrm{i}a^{-\frac{1}{2}}} \end{bmatrix},$$

$|\xi| \geq 1$ and $\mathrm{Im}\{\xi\} \leq 0$.

Once the two analytic functions have been derived, the mode-III stress intensity factors K_{III}^L, K_{III}^R and K_{III}^D at the three crack tips $z = 1/a$, $z = a$ and $z = \exp(\mathrm{i}\theta_0)$ can be concisely given by

$$(5.5) \quad K_{\mathrm{III}}^L = \frac{\mu_1\mu_2 b}{\mu_1+\mu_2}\sqrt{\frac{a}{2\pi(a^2-1)}}$$
$$\times \left[\begin{array}{l} a - 1 - \mathrm{Re}\left\{(1-\mathrm{i}a^{\frac{1}{2}})\sqrt{(\mathrm{i}a^{\frac{1}{2}}-\mathrm{e}^{\mathrm{i}\psi})(\mathrm{i}a^{\frac{1}{2}}-\mathrm{e}^{-\mathrm{i}\psi})}\right\} \\[1em] + a^{\frac{1}{2}}\mathrm{Im}\left\{\xi_0+\xi_0^{-1}-(1-\xi_0^{-1})\sqrt{(\xi_0-\mathrm{e}^{\mathrm{i}\psi})(\xi_0-\mathrm{e}^{-\mathrm{i}\psi})}\right\} \end{array} \right],$$

$$(5.6) \quad K_{\mathrm{III}}^R = \frac{\mu_1\mu_2 b}{\mu_1+\mu_2}\frac{1}{\sqrt{2\pi(a^3-a)}}$$
$$\times \left[\begin{array}{l} \dfrac{\mu_2}{\mu_1}(a-1) + \mathrm{Re}\left\{(1-\mathrm{i}a^{\frac{1}{2}})\sqrt{(\mathrm{i}a^{\frac{1}{2}}-\mathrm{e}^{\mathrm{i}\psi})(\mathrm{i}a^{\frac{1}{2}}-\mathrm{e}^{-\mathrm{i}\psi})}\right\} \\[1em] + a^{\frac{1}{2}}\mathrm{Im}\left\{\dfrac{\mu_2}{\mu_1}(\xi_0+\xi_0^{-1}) + (1-\xi_0^{-1})\sqrt{(\xi_0-\mathrm{e}^{\mathrm{i}\psi})(\xi_0-\mathrm{e}^{-\mathrm{i}\psi})}\right\} \end{array} \right],$$

$$(5.7) \quad K_{\mathrm{III}}^D = \frac{\mu_1\mu_2 b}{\mu_1+\mu_2}\frac{\sqrt{a^2+1+2a\cos 2\psi}}{\sqrt{\pi(a^2-1)\tan\frac{\psi}{2}}}$$
$$\times \mathrm{Im}\left\{ \frac{1-\mathrm{i}a^{\frac{1}{2}}}{\sqrt{(\mathrm{i}a^{\frac{1}{2}}-\mathrm{e}^{\mathrm{i}\psi})(\mathrm{i}a^{\frac{1}{2}}-\mathrm{e}^{-\mathrm{i}\psi})}} + \frac{1-\xi_0}{\sqrt{(\xi_0-\mathrm{e}^{\mathrm{i}\psi})(\xi_0-\mathrm{e}^{-\mathrm{i}\psi})}} \right\},$$

from which the following identity can be derived:

$$K_{III}^{L} + aK_{III}^{R} = \mu_2 b \sqrt{\frac{a}{2\pi(a^2-1)}} \left[a - 1 + a^{\frac{1}{2}} \, \text{Im} \left\{ \xi_0 + \xi_0^{-1} \right\} \right]$$

$$= \mu_2 b \sqrt{\frac{a}{2\pi(a^2-1)}} \left[a - 1 + \left(\sqrt{\frac{r_1}{r_2}} - a\sqrt{\frac{r_2}{r_1}} \right) \cos \frac{\theta_1 - \theta_2}{2} \right],$$

where $z_0 - a = r_1 \exp(i\theta_1)$ and $z_0 - 1/a = r_2 \exp(i\theta_2)$, as shown in Fig. 1. The above identity indicates that the sum $(K_{III}^{L} + aK_{III}^{R})$ is independent of the shear modulus μ_1 of the inhomogeneity, and the length of the arc crack L_c. By letting $\text{Im}\{\xi_0\} \to 0^-$ or by letting $|\xi_0| = 1$ and $-\pi < \arg(\xi_0) < -\psi$ (i.e., by letting the screw dislocation approach the crack surfaces), Eqs. (5.5)–(5.7) reduce to Eqs. (5.1)–(5.3).

When $\psi = \pi$ (or equivalently $\theta_0 = 0$) for a finite Griffith crack penetrating a perfectly bonded circular inhomogeneity, Eqs. (5.5) and (5.6) become

$$K_{III}^{L} = -\frac{2\mu_1\mu_2 b}{\mu_1 + \mu_2} \sqrt{\frac{a}{2\pi(a^2-1)}} \left[1 - \sqrt{\frac{r_1}{r_2}} \cos \frac{\theta_1 - \theta_2}{2} \right],$$

$$K_{III}^{R} = \mu_2 b \sqrt{\frac{a}{2\pi(a^2-1)}}$$

$$\times \left[1 + a^{-1} \frac{\mu_1 - \mu_2}{\mu_1 + \mu_2} - \left(\sqrt{\frac{r_2}{r_1}} + a^{-1} \frac{\mu_1 - \mu_2}{\mu_1 + \mu_2} \sqrt{\frac{r_1}{r_2}} \right) \cos \frac{\theta_1 - \theta_2}{2} \right],$$

which also recovers recent results in [14, 15].

5.3. A screw dislocation in the inhomogeneity

We consider a screw dislocation with Burgers vector b located at $z = z_0$, $(|z_0| < 1)$ in the inhomogeneity (or $\xi = \xi_0 = -\sqrt{(1 - az_0)/(z_0 - a)}$, $(|\xi_0| < 1)$ in the ξ-plane). The two analytic functions $f_1'(\xi)$ and $f_2'(\xi)$ for this loading case can be derived as

$$f_1'(\xi) = \frac{\mu_1 b}{2\pi(\mu_1 + \mu_2)} \left[\frac{1}{\xi - \xi_0} - \frac{1}{\xi - \bar{\xi}_0} - \frac{1}{\xi - \bar{\xi}_0^{-1}} + \frac{1}{\xi - \xi_0^{-1}} \right]$$

$$- \frac{\mu_2 b}{2\pi(\mu_1 + \mu_2)} \left[\frac{1}{\xi + ia^{\frac{1}{2}}} - \frac{1}{\xi - ia^{\frac{1}{2}}} - \frac{1}{\xi + ia^{-\frac{1}{2}}} + \frac{1}{\xi - ia^{-\frac{1}{2}}} \right]$$

$$+ \frac{\mu_2 b}{2\pi(\mu_1 + \mu_2)\sqrt{(\xi - e^{i\psi})(\xi - e^{-i\psi})}}$$

$$
\times \left[
\begin{array}{l}
\dfrac{\sqrt{(\xi_0 - e^{i\psi})(\xi_0 - e^{-i\psi})}}{\xi - \xi_0} - \dfrac{\sqrt{(\bar{\xi}_0 - e^{i\psi})(\bar{\xi}_0 - e^{-i\psi})}}{\xi - \bar{\xi}_0} \\[3mm]
+ \dfrac{\sqrt{(\bar{\xi}_0^{-1} - e^{i\psi})(\bar{\xi}_0^{-1} - e^{-i\psi})}}{\xi - \bar{\xi}_0^{-1}} - \dfrac{\sqrt{(\xi_0^{-1} - e^{i\psi})(\xi_0^{-1} - e^{-i\psi})}}{\xi - \xi_0^{-1}} \\[3mm]
- \dfrac{\sqrt{(-ia^{\frac{1}{2}} - e^{i\psi})(-ia^{\frac{1}{2}} - e^{-i\psi})}}{\xi + ia^{\frac{1}{2}}} + \dfrac{\sqrt{(ia^{\frac{1}{2}} - e^{i\psi})(ia^{\frac{1}{2}} - e^{-i\psi})}}{\xi - ia^{\frac{1}{2}}} \\[3mm]
- \dfrac{\sqrt{(-ia^{-\frac{1}{2}} - e^{i\psi})(-ia^{-\frac{1}{2}} - e^{-i\psi})}}{\xi + ia^{-\frac{1}{2}}} + \dfrac{\sqrt{(ia^{-\frac{1}{2}} - e^{i\psi})(ia^{-\frac{1}{2}} - e^{-i\psi})}}{\xi - ia^{-\frac{1}{2}}}
\end{array}
\right],
$$

$|\xi| \leq 1$ and $\text{Im}\{\xi\} \leq 0$;

$$
f_2'(\xi) = \frac{\mu_1 b}{2\pi(\mu_1 + \mu_2)} \left[\frac{1}{\xi - \xi_0} - \frac{1}{\xi - \bar{\xi}_0} - \frac{1}{\xi - \bar{\xi}_0^{-1}} + \frac{1}{\xi - \xi_0^{-1}} \right]
$$

$$
- \frac{\mu_2 b}{2\pi(\mu_1 + \mu_2)} \left[\frac{1}{\xi + ia^{\frac{1}{2}}} - \frac{1}{\xi - ia^{\frac{1}{2}}} - \frac{1}{\xi + ia^{-\frac{1}{2}}} + \frac{1}{\xi - ia^{-\frac{1}{2}}} \right]
$$

$$
+ \frac{\mu_1 b}{2\pi(\mu_1 + \mu_2)\sqrt{(\xi - e^{i\psi})(\xi - e^{-i\psi})}}
$$

$$
\times \left[
\begin{array}{l}
\dfrac{\sqrt{(\xi_0 - e^{i\psi})(\xi_0 - e^{-i\psi})}}{\xi - \xi_0} - \dfrac{\sqrt{(\bar{\xi}_0 - e^{i\psi})(\bar{\xi}_0 - e^{-i\psi})}}{\xi - \bar{\xi}_0} \\[3mm]
+ \dfrac{\sqrt{(\bar{\xi}_0^{-1} - e^{i\psi})(\bar{\xi}_0^{-1} - e^{-i\psi})}}{\xi - \bar{\xi}_0^{-1}} - \dfrac{\sqrt{(\xi_0^{-1} - e^{i\psi})(\xi_0^{-1} - e^{-i\psi})}}{\xi - \xi_0^{-1}} \\[3mm]
- \dfrac{\sqrt{(-ia^{\frac{1}{2}} - e^{i\psi})(-ia^{\frac{1}{2}} - e^{-i\psi})}}{\xi + ia^{\frac{1}{2}}} + \dfrac{\sqrt{(ia^{\frac{1}{2}} - e^{i\psi})(ia^{\frac{1}{2}} - e^{-i\psi})}}{\xi - ia^{\frac{1}{2}}} \\[3mm]
- \dfrac{\sqrt{(-ia^{-\frac{1}{2}} - e^{i\psi})(-ia^{-\frac{1}{2}} - e^{-i\psi})}}{\xi + ia^{-\frac{1}{2}}} + \dfrac{\sqrt{(ia^{-\frac{1}{2}} - e^{i\psi})(ia^{-\frac{1}{2}} - e^{-i\psi})}}{\xi - ia^{-\frac{1}{2}}}
\end{array}
\right],
$$

$|\xi| \geq 1$ and $\text{Im}\{\xi\} \leq 0$.

Once these two analytic functions have been identified, the mode-III stress intensity factors K_{III}^L, K_{III}^R and K_{III}^D at the three crack tips $z = 1/a$, $z = a$ and $z = \exp(i\theta_0)$ are given by

(5.8) $K_{\mathrm{III}}^{L} = \dfrac{\mu_1\mu_2 b}{\mu_1 + \mu_2}\sqrt{\dfrac{a}{2\pi(a^2-1)}}$

$$\times\left[\begin{array}{l} a - 1 - \mathrm{Re}\left\{(1 - \mathrm{i}a^{\frac{1}{2}})\sqrt{(\mathrm{i}a^{\frac{1}{2}} - \mathrm{e}^{\mathrm{i}\psi})(\mathrm{i}a^{\frac{1}{2}} - \mathrm{e}^{-\mathrm{i}\psi})}\right\} \\ +a^{\frac{1}{2}}\mathrm{Im}\left\{\dfrac{\mu_1}{\mu_2}(\xi_0 + \xi_0^{-1}) - (1 - \xi_0^{-1})\sqrt{(\xi_0 - \mathrm{e}^{\mathrm{i}\psi})(\xi_0 - \mathrm{e}^{-\mathrm{i}\psi})}\right\} \end{array}\right],$$

(5.9) $K_{\mathrm{III}}^{R} = \dfrac{\mu_1\mu_2 b}{\mu_1 + \mu_2}\dfrac{1}{\sqrt{2\pi(a^3-a)}}$

$$\times\left[\begin{array}{l} \dfrac{\mu_2}{\mu_1}(a - 1) + \mathrm{Re}\left\{(1 - \mathrm{i}a^{\frac{1}{2}})\sqrt{(\mathrm{i}a^{\frac{1}{2}} - \mathrm{e}^{\mathrm{i}\psi})(\mathrm{i}a^{\frac{1}{2}} - \mathrm{e}^{-\mathrm{i}\psi})}\right\} \\ +a^{\frac{1}{2}}\mathrm{Im}\left\{\xi_0 + \xi_0^{-1} + (1 - \xi_0^{-1})\sqrt{(\xi_0 - \mathrm{e}^{\mathrm{i}\psi})(\xi_0 - \mathrm{e}^{-\mathrm{i}\psi})}\right\} \end{array}\right],$$

(5.10) $K_{\mathrm{III}}^{D} = \dfrac{\mu_1\mu_2 b}{\mu_1 + \mu_2}\dfrac{\sqrt{a^2 + 1 + 2a\cos 2\psi}}{\sqrt{\pi(a^2-1)\tan\frac{\psi}{2}}}$

$$\times\mathrm{Im}\left\{\dfrac{1 - \mathrm{i}a^{\frac{1}{2}}}{\sqrt{(\mathrm{i}a^{\frac{1}{2}} - \mathrm{e}^{\mathrm{i}\psi})(\mathrm{i}a^{\frac{1}{2}} - \mathrm{e}^{-\mathrm{i}\psi})}} + \dfrac{1 - \xi_0}{\sqrt{(\xi_0 - \mathrm{e}^{\mathrm{i}\psi})(\xi_0 - \mathrm{e}^{-\mathrm{i}\psi})}}\right\},$$

from which we find that

(5.11) $K_{\mathrm{III}}^{L} + a K_{\mathrm{III}}^{R}$

$$= b\sqrt{\dfrac{a}{2\pi(a^2-1)}}\left[\mu_2(a-1) + \mu_1 a^{\frac{1}{2}}\mathrm{Im}\left\{\xi_0 + \xi_0^{-1}\right\}\right]$$

$$= b\sqrt{\dfrac{a}{2\pi(a^2-1)}}\left[\mu_2(a-1) + \mu_1\left(\sqrt{\dfrac{r_1}{r_2}} - a\sqrt{\dfrac{r_2}{r_1}}\right)\cos\dfrac{\theta_1 - \theta_2}{2}\right].$$

Equation (5.11) indicates that the sum $(K_{\mathrm{III}}^{L} + a K_{\mathrm{III}}^{R})$ is independent of the length of the arc crack L_c. By letting $\mathrm{Im}\{\xi_0\} \to 0^{-}$ or by letting $|\xi_0| = 1$ and $-\pi < \arg(\xi_0) < -\psi$ (i.e., by letting the screw dislocation approach the crack surfaces), Eqs. (5.8)–(5.10) will reduce to Eqs. (5.1)–(5.3).

When $\psi = \pi$ (or equivalently $\theta_0 = 0$) for a finite Griffith crack penetrating a perfectly bonded circular inhomogeneity, Eqs. (5.8) and (5.9) become

$$K_{\mathrm{III}}^{L} = -\mu_1 b\sqrt{\dfrac{a}{2\pi(a^2-1)}}\left[\dfrac{2\mu_2}{\mu_1 + \mu_2} + \left(a\dfrac{\mu_1 - \mu_2}{\mu_1 + \mu_2}\sqrt{\dfrac{r_2}{r_1}} - \sqrt{\dfrac{r_1}{r_2}}\right)\cos\dfrac{\theta_1 - \theta_2}{2}\right],$$

$$K_{\mathrm{III}}^{R} = \mu_2 b\sqrt{\dfrac{a}{2\pi(a^2-1)}}\left[1 + a^{-1}\dfrac{\mu_1 - \mu_2}{\mu_1 + \mu_2} - \dfrac{2\mu_1}{\mu_1 + \mu_2}\sqrt{\dfrac{r_2}{r_1}}\cos\dfrac{\theta_1 - \theta_2}{2}\right],$$

which again recovers the results in [14, 15].

Finally, we consider two special locations of the screw dislocation. Firstly, if the dislocation is located at the center of the circular inhomogeneity, or equivalently $\xi_0 = -ia^{-1/2}$, Eqs. (5.5)–(5.7) become

$$\frac{K_{\text{III}}^L}{\mu_1} = \frac{aK_{\text{III}}^R}{\mu_2} = b\sqrt{\frac{a(a-1)}{2\pi(a+1)}}, \qquad K_{\text{III}}^D = 0,$$

which indicates that the length of the arc crack L_c exerts no influence on these stress intensity factors and that the induced stress intensity factor at the arc crack tip is zero.

Next, if the dislocation is just on the bonded part of the circular interface, it follows from either Eqs. (5.8)–(5.10) for a dislocation in the matrix or Eqs. (5.5)–(5.7) for a dislocation in the inhomogeneity that

$$K_{\text{III}}^L = \frac{\mu_1\mu_2 b}{\mu_1 + \mu_2}\sqrt{\frac{a}{2\pi(a^2-1)}}$$
$$\times \left[\begin{array}{l} a - 1 - \text{Re}\left\{(1 - ia^{\frac{1}{2}})\sqrt{(ia^{\frac{1}{2}} - e^{i\psi})(ia^{\frac{1}{2}} - e^{-i\psi})}\right\} \\ -2a^{\frac{1}{2}}\,\text{Im}\left\{\sqrt{(\xi_0 - e^{i\psi})(\xi_0 - e^{-i\psi})}\right\} \end{array}\right],$$

$$K_{\text{III}}^R = \mu_2 b\sqrt{\frac{a-1}{2\pi a(a+1)}} - a^{-1}K_{\text{III}}^L,$$

$$K_{\text{III}}^D = \frac{\mu_1\mu_2 b}{\mu_1 + \mu_2}\frac{\sqrt{a^2 + 1 + 2a\cos 2\psi}}{\sqrt{\pi(a^2-1)\tan\frac{\psi}{2}}}$$
$$\times \text{Im}\left\{\frac{1 - ia^{\frac{1}{2}}}{\sqrt{(ia^{\frac{1}{2}} - e^{i\psi})(ia^{\frac{1}{2}} - e^{-i\psi})}} + \frac{2}{\sqrt{(\xi_0 - e^{i\psi})(\xi_0 - e^{-i\psi})}}\right\},$$

where $|\xi_0| = 1$ and $-\psi < \arg(\xi_0) < \psi$. Interestingly, in this special case, the expression of the sum $(K_{\text{III}}^L + aK_{\text{III}}^R)$ is identical to Eq. (5.4) for a Zener–Stroh crack.

6. Conclusions

We perform a rigorous and analytical study of a radial matrix crack penetrating a partially debonded circular inhomogeneity under longitudinal shear. We first consider in detail the loading case in which the matrix is subjected to remote uniform shear stresses. The mode-III stress intensity factors K_{III}^L, K_{III}^R and K_{III}^D at the three crack tips $z = 1/a$, $z = a$ and $z = \exp(i\theta_0)$ are obtained in Eqs. (3.1)–(3.3). The displacement jumps across the two surfaces of

the radial matrix crack and across those of the arc interface crack are given by Eqs. (3.5)–(3.7). The influence of the length of the arc interface crack and that of the straight matrix crack on the variations of the stress intensity factors and on displacement jumps is visually illustrated in Figs. 3–10. The stress intensity factors for three other loading cases are obtained in Eqs. (5.1)–(5.3) for a Zener–Stroh crack, (5.5)–(5.7) for a screw dislocation in the matrix and (5.8)–(5.10) for a screw dislocation in the inhomogeneity. We derive identities involving $(K_{\mathrm{III}}^{L} + aK_{\mathrm{III}}^{R})$ for all the four loading cases and find that they are always independent of the length of the arc crack L_c.

Acknowledgements

References

1. A.H. England, *An arc crack around a circular elastic inclusion*, J. Appl. Mech. (ASME), **33**, 637–640, 1966.

2. F. Erdogan, G.D. Gupta, *The inclusion problem with a crack crossing the boundary*, Int. J. Fract., **11**, 13–27, 1975.

3. J.W. Hutchinson, *Stresses and failure modes in thin films and multilayers*, Lecture Notes, 1996.

4. C.I. Kim, P. Schiavone, C.-Q. Ru, *The effect of surface elasticity on a Mode-III interface crack*, Arch. Mech., **63**, 3, 267–286, 2011.

5. Y. Liu, C.-Q. Ru, P. Schiavone, A. Mioduchowski, *New phenomena concerning the effect of imperfect bonding on radial matrix cracking in fiber composites*, Int. J. Engng. Sci., **39**, 2033–2050, 2001.

6. N.I. Muskhelishvili, *Some Basic Problems of the Mathematical Theory of Elasticity*, Noordhoff Ltd., Netherlands, 1963.

7. A.B. Perlman, G.C. Sih, *Elastostatic problems of curvilinear cracks in bonded dissimilar materials*, Int. J. Eng. Sci., **5**, 845–867, 1967.

8. M. Vasudevan, P. Schiavone, *New results concerning the identification of neutral inhomogeneities in plane elasticity*, Arch. Mech., **58**, 1, 45–58, 2006.

9. P.S. Steif, *A semi-infinite crack partially penetrating a circular inclusion*, J. Appl. Mech., **54**, 87–93, 1987.

10. A.N. Stroh, *The formation of cracks as a result of plastic flow, I*, Proc. Roy. Soc. Lond., A **223**, 404–414, 1954.

11. O. Tamate, T. Yamada, *Stresses in an infinite body with a partially bonded circular cylindrical inclusion under longitudinal shear*, Technology Reports, Tohoku University, **34**, 161, 1969.

12. M. TOYA, *Crack along interface of a circular inclusion embedded in an infinite solid*, J. Mech. Phys. Solids, **22**, 325–348, 1974.

13. Y.P. WANG, R. BALLARINI, *A long crack penetrating a circular inhomogeneity*, Meccanica, **38**, 579–593, 2003.

14. X. WANG, E. PAN, W.J. FENG, *Closed-form solutions for a mode III radial matrix crack penetrating a circular inhomogeneity*, Appl. Math. Model., **32**, 2925–2935, 2008.

15. X. WANG, E. PAN, *On a finite crack partially penetrating two circular inhomogeneities and some related problems*, Appl. Math. Model., DOI 10.1016/j.apm.2011.09.014 [to appear].

16. C. ZENER, *The micro-mechanism of fracture*, Fracturing of metals, American Society for Metals, Cleveland, 3–31, 1948.